Online Research @ Cardiff

This is an Open Access document downloaded from ORCA, Cardiff University's institutional repository: https://orca.cardiff.ac.uk/id/eprint/118218/

This is the author's version of a work that was submitted to / accepted for publication.

Citation for final published version:

Yahui, Zhang, Yuyin, Li and Kennedy, David ORCID: https://orcid.org/0000-0002-8837-7296 2019. An uncertain computational model for random vibration analysis of subsea pipelines subjected to spatially varying ground motions. Engineering Structures 183 , pp. 550-561. 10.1016/j.engstruct.2019.01.031 file

Publishers page: http://dx.doi.org/10.1016/j.engstruct.2019.01.031 <http://dx.doi.org/10.1016/j.engstruct.2019.01.031>

Please note:
Changes made as a result of publishing processes such as copy-editing, formatting and page numbers may not be reflected in this version. For the definitive version of this publication, please refer to the published source. You are advised to consult the publisher's version if you wish to cite this paper.

This version is being made available in accordance with publisher policies. See http://orca.cf.ac.uk/policies.html for usage policies. Copyright and moral rights for publications made available in ORCA are retained by the copyright holders.

information services
gwasanaethau gwybodaeth

An Uncertain Computational Model for Random Vibration Analysis of Subsea Pipelines Subjected to Spatially Varying Ground Motions

Yahui Zhang[a*], Yuyin Li[a], David Kennedy[b]

[a] *State Key Laboratory of Structural Analysis for Industrial Equipment, Department of Engineering Mechanics, International Center for Computational Mechanics, Dalian University of Technology, Dalian 116023, PR China;*

[b] *School of Engineering, Cardiff University, Cardiff CF24 3AA, Wales, UK*

Corresponding author:

Dr. Y. H. Zhang

State Key Laboratory of Structural Analysis for Industrial Equipment, Department of Engineering Mechanics, Dalian University of Technology, Dalian 116023, PR China

Email: zhangyh@dlut.edu.cn

Tel: +86 411 84706337

Fax: +86 411 84708393

Abstract

Based on a nonparametric modelling approach, this paper presents a random vibration analysis of a subsea pipeline subjected to spatially varying ground motions. The earthquake-induced ground motions are modelled as nonstationary random processes and their spatial variations are considered. The modelling uncertainties of the subsea pipeline are taken into account using a random matrix theory, while the unilateral contact relationship between the pipeline and seabed is also considered. Thus, an uncertain computational model for the subsea pipeline subjected to a random earthquake is established, and the corresponding solutions are calculated using Monte Carlo simulation (MCS). In order to highlight the contribution of the unilateral contact effect to random responses of pipelines, comparative studies are performed between the unilateral and permanent contact models. In numerical examples, the possible convergence problems in the present computational model are firstly studied to determine the optimal numbers of reduced modes and MCS samples. Then influences of the randomness in the earthquake and modelling uncertainties in the pipeline are investigated qualitatively through three representative cases. The different propagations of randomness and modelling uncertainties in the unilateral and permanent models are also examined and discussed. It is concluded that the randomness of the earthquake and modelling uncertainties of the pipeline have significant influences on the statistical characteristics of earthquake responses of the pipeline.

Keywords: modelling uncertainty; random earthquake; subsea pipeline; spatially varying ground motions; unilateral contact

1 Introduction

The subsea pipeline is an important part of offshore oil and gas exploitation systems. When a pipeline is broken, the ocean environment might be polluted and underwater repair is very difficult and costly. Earthquakes are typical environmental excitations during the service life of the pipeline. As an occasional random excitation, an earthquake poses a tremendous threat to the safety of the pipeline, and hence the dynamic problem of the pipeline under an earthquake has received great attention. Due to the high cost and technical difficulties of experiments, the earthquake analysis and design of the pipeline are mainly based on numerical simulations. Thus, establishing an accurate numerical computational model is of great significance to the earthquake analysis of the pipeline. On the other hand, there are inevitably randomness and uncertainties in this computational model on account of the natural random factors and lack of relevant data. This paper discusses how to introduce randomness and uncertainties into the computational model and how they influence the system response.

For reasons of manufacturing errors and corrosion, some physical and geometric parameters of the pipeline, such as Young's modulus, mass density, wall thickness etc., may be uncertain. These parameters can be considered as random variables and their uncertainties are usually characterized by probability distribution functions. Spatial

correlations of these parameters can be further considered by using the random field theory. Uncertainties introduced by random variables or fields are called data uncertainties and this quantification approach is usually termed the parametric uncertainty approach. This approach has been successfully applied to model uncertainties in many different static and dynamic structural analyses [1-5]. Meanwhile, there is another kind of uncertainty, known as modelling uncertainty, in the dynamic analysis of the pipeline. The modelling uncertainty stems primarily from two sources. The first source is the simplifying assumptions invoked when developing a mathematical model. For instance, when dealing with a beam structure, the use of beam theory instead of three dimensional elasticity theory introduces a reduced admissible displacement field. The second source is the unquantified errors associated with the modelling of structural joints or connections. For example, the pipeline consists of many welding points and bolted connections, whose properties are always uncertain and depend on many parameters. Since the modelling uncertainty contains too many uncertain parameters, some of which cannot even be identified, it is difficult to quantify it by the parametric uncertainty approach.

To deal with the modelling uncertainty, a nonparametric approach based on random matrix theory was developed by Soize [6]. In the framework of the nonparametric approach, the generalized mass, damping and stiffness matrices of the reduced matrix model are replaced by corresponding random matrices. Then the probability distribution functions of these random matrices are constructed using Jaynes' entropy with the

80 constraints defined by some available information. For random matrix models of the
81 system, it is not necessary to identify which system parameters are uncertain or their
82 detailed distribution information, while the global dispersion level of each random matrix
83 can be controlled by a unique positive parameter called the dispersion parameter. Hence,
84 this approach is very suitable for dealing with the modelling uncertainty introduced by
85 the unavoidable approximation and simplification of unknown and imprecise expression
86 of a complex structure in establishing a mathematical equation from a physical structure.
87 The main theoretical concepts and derivation procedures of the nonparametric approach
88 are presented in [6, 7]. This approach is also validated by several experiments, such as a
89 model consisting of two rectangular plates connected together with a complex joint [8, 9],
90 a cantilever plate with randomly attached spring-mass oscillators [10], post-buckling of a
91 thin cylindrical shell submitted to a static shear load [11], and so on. To date, this approach
92 has been applied to various industrial problems, for example the random vibration and
93 reliability analysis of complex aerospace engineering systems [12, 13], the dynamic
94 behaviour prediction of an uncertain Jeffcott rotor with disc offset [14], the vibration
95 analysis of a drill-string with bit-rock interaction [15], and so on. To the authors'
96 knowledge, the literature contains many studies on the data uncertainty but far fewer on
97 the modelling uncertainty, and so the focus of this paper is on modelling uncertainty in
98 the dynamic analysis of subsea pipelines.

99 The data and modelling uncertainties mentioned above come from the structure itself.

Nevertheless, ground motions caused by the earthquake are also uncertain due to the natural randomness of soil and the complex propagation mechanism of earthquake waves. Uncertainties of the earthquake are usually characterized by random processes [16]. Meanwhile, spatial variations can be found in earthquake waves propagating along long-span structures, such as subsea pipelines, which result in differences in the amplitude and phase of ground motions at the supports of the structures. This phenomenon is known as spatially varying ground motions [17]. Such spatial variations have been considered in earthquake analysis of many long-span structures, such as a multi-supported suspension bridge [18], supporting towers of overhead electricity transmission systems [19], dam-reservoir-foundation systems [20], etc., and their influences on the random earthquake responses of long-span structures are recognized to be significant.

In the dynamic analysis of subsea pipelines, one key point is how to consider the relationship between pipelines and the seabed as exactly as possible. For reasons of high costs and construction difficulties, subsea pipelines always rest freely on the seabed, rather than being buried or anchored. In the literature on the dynamic analysis of unburied pipelines, pipelines are usually modelled as beams permanently contacted with elastic foundations [21-25]. However, in reality unburied pipelines are constrained unilaterally by the seabed, which means that the reaction of the seabed can only be compressive and not tensile. Hence, during the vibration of pipelines, particularly when the deformation takes place predominantly in the vertical plane, a separation of pipelines and the seabed

120 will occur. Clearly, the elastic foundation beam model will overestimate the constraint
121 between pipelines and the seabed. To overcome this drawback of the elastic foundation
122 beam model, a unilateral contact model is used in this paper to simulate the relationship
123 between subsea pipelines and the seabed. Note that the unilateral contact model will
124 inevitably introduce nonlinearity into the random analysis, and hence Monte Carlo
125 simulation (MCS) seems to be the best and only method to obtain random responses of
126 pipelines. Fortunately, the implementation of the nonparametric approach mentioned
127 above is based on MCS, and so the contact nonlinearity does not incur any additional
128 computational requirements.

129 This paper studies the random vibration of subsea pipelines subjected to spatially
130 varying ground motions, considering the randomness of the earthquake and the modelling
131 uncertainties of the pipeline. The paper is organized as follows. Section 2 gives the
132 mathematical formulation of a subsea pipeline under an earthquake, and then presents the
133 finite element model and the corresponding reduced computational model. In section 3,
134 quantification approaches and simulation strategies for modelling uncertainties of the
135 pipeline are given. Section 4 presents some numerical examples. Convergence analyses
136 are firstly performed with respect to the dimension of the reduced models and the number
137 of MCS samples. Then propagations of randomness and modelling uncertainties in the
138 present computational model are investigated qualitatively through three representative
139 cases. Finally, concluding remarks are made in section 5.

2 Deterministic modelling of the subsea pipeline subjected to ground motions

2.1 Governing equations of the pipeline

Fig. 1 shows a typical subsea pipeline subjected to an earthquake. The dashed part represents the initial profile of the subsea pipeline and seabed before the earthquake, while the solid part represents the deformed profile during the earthquake.

The subsea pipeline is simplified as a Timoshenko beam, and hydrodynamic forces caused by the internal oil and the surrounding sea water are considered. According to the fluid-conveying beam theory [26] and Morison's equation for slender cylindrical structures [27], governing equations of the subsea pipeline in the vertical plane can be written as

$$\begin{aligned}
&(\rho I + \rho_{\text{oil}} I_{\text{oil}})\frac{\partial^2 \theta}{\partial t^2} - EI\frac{\partial^2 \theta}{\partial x^2} - \kappa GA\left(\frac{\partial w}{\partial x} - \theta\right) = 0 \\
&\left(m_{\text{pipe}} + m_{\text{oil}} + m_{\text{water}}\right)\frac{\partial^2 w}{\partial t^2} + \left(m_{\text{oil}} v_{\text{oil}}^2 + N_0 - \kappa GA\right)\frac{\partial^2 w}{\partial x^2} \\
&+ 2m_{\text{oil}} v_{\text{oil}}\frac{\partial^2 w}{\partial x \partial t} + \kappa GA\frac{\partial \theta}{\partial x} = -f_{\text{seabed}}
\end{aligned} \tag{1}$$

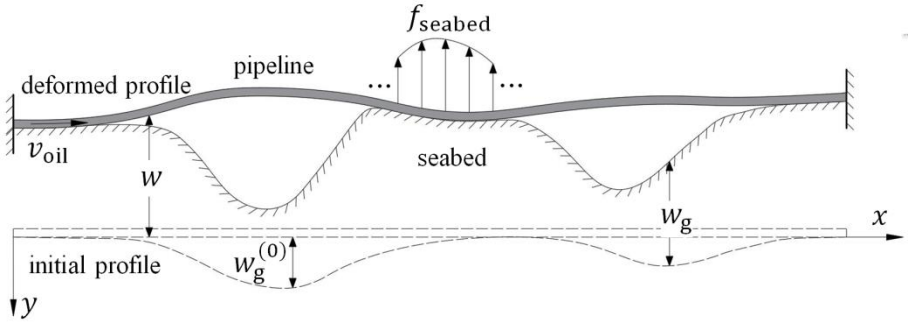

Fig. 1 Schematic of subsea pipeline and seabed

where x and t are respectively the position and time; θ and w are respectively the cross-section rotation and vertical displacement of the pipeline; ρI and $\rho_{\mathrm{oil}} I_{\mathrm{oil}}$ are respectively the moments of inertia of the pipeline and oil; EI and κGA are respectively the flexural and effective shear rigidity of the pipeline; m_{pipe}, m_{oil} and m_{water} are the masses of the pipeline, oil and additional water per unit length; v_{oil} is the flow velocity of the oil which is assumed to be a constant; N_0 is the axial compression; f_{seabed} is the reaction force per unit length of the seabed.

Ignoring the friction of the seabed and considering unilateral contact of the seabed and pipeline, the reaction force of the seabed f_{seabed} can be expressed as

$$f_{\mathrm{seabed}} = \begin{cases} 0 & \xi > 0 \\ \eta k_{\mathrm{seabed}} & \xi = 0 \end{cases} \tag{2}$$

where k_{seabed} is the stiffness of the seabed, and

$$\xi = \eta + w_{\mathrm{g}}^{(0)} + w_{\mathrm{g}} - w \tag{3}$$

is the relative displacement between the pipeline and seabed, $w_{\mathrm{g}}^{(0)}$ is the initial seabed profile, η is the compressional deformation of the seabed and w_{g} is the motion of the seabed.

2.2 Discretization by finite elements

Due to the contact nonlinearity, it is very difficult to obtain an analytical solution of Eq. (1). Hence, a numerical solution using the finite element method seems to be the only

choice. Timoshenko beam elements with two nodes are used to discretize the pipeline. Since effects of the oil conveyed through the pipeline and the surrounding seawater are considered, the beam element used in this paper is different from the conventional one. Therefore, a brief derivation of the finite element formulation is given here.

The displacement field within a beam element can be interpolated as [28]

$$w = \boldsymbol{N}\boldsymbol{q}_{\mathrm{e}}, \qquad \theta = \bar{\boldsymbol{N}}\boldsymbol{q}_{\mathrm{e}} \tag{4}$$

in which $\boldsymbol{q}_{\mathrm{e}}$ is the 4×1 node displacement vector, $\boldsymbol{N}$ and $\bar{\boldsymbol{N}}$ denote 1×4 shape function vectors, which can be written as

$$\begin{aligned} \boldsymbol{N} &= [N_1 \quad N_2 \quad N_3 \quad N_4] \\ \bar{\boldsymbol{N}} &= [\bar{N}_1 \quad \bar{N}_2 \quad \bar{N}_3 \quad \bar{N}_4] \end{aligned} \tag{5}$$

where

$$\begin{aligned} N_1 &= 1 - \frac{1}{l(l^2+12g)}(12g\chi + 3l\chi^2 - 2\chi^3) \\ N_2 &= \frac{1}{l(l^2+12g)}[(l^2+6g)l\chi - (2l^2+6g)\chi^2 + l\chi^3] \\ N_3 &= \frac{1}{l(l^2+12g)}(12g\chi + 3l\chi^2 - 2\chi^3) \\ N_4 &= \frac{1}{l(l^2+12g)}[-6gl\chi + (6g-l^2)\chi^2 + l\chi^3] \\ \bar{N}_1 &= \frac{1}{l(l^2+12g)}(6\chi^2 - 6l\chi) \\ \bar{N}_2 &= \frac{1}{l(l^2+12g)}[l^3 + 12gl - (4l^2+12g)\chi + 3l\chi^2] \\ \bar{N}_3 &= \frac{1}{l(l^2+12g)}(6l\chi - 6\chi^2) \end{aligned} \tag{6}$$

$$\bar{N}_4 = \frac{1}{l(l^2+12g)}[3l\chi^2 - (2l^2-12g)\chi]$$

189

190 where l is the element length, χ is the local coordinate and $g = EI/(\kappa GA)$.

191 The shear strain of the beam cross section can be written as

192

$$\gamma = \frac{\partial w}{\partial x} - \theta \tag{7}$$

193

194 Hence the strain energy and kinetic energy of a beam element can be expressed as

195

$$V_{\mathrm{e}} = \frac{1}{2}\int_0^a \left[EI\left(\frac{\partial\theta}{\partial x}\right)^2 + \kappa GA\gamma^2 + N_0\left(\frac{\partial w}{\partial x}\right)^2\right]\mathrm{d}\,\chi$$

$$T_{\mathrm{e}} = \frac{1}{2}\int_0^a \left[(\rho I + \rho_{\mathrm{oil}} I_{\mathrm{oil}})\left(\frac{\partial\theta}{\partial t}\right)^2 + (m_{\mathrm{pipe}} + m_{\mathrm{water}})\left(\frac{\partial w}{\partial t}\right)^2 + m_{\mathrm{oil}} v_{\mathrm{oil}}^2\right. \tag{8}$$

$$\left. + m_{\mathrm{oil}}\left(\frac{\partial w}{\partial t} + v_{\mathrm{oil}}\frac{\partial w}{\partial x}\right)^2\right]\mathrm{d}\,\chi$$

196

197 According to the variational principle, the element matrices can be obtained directly

198 by substituting Eq. (4) into Eq. (8),

199

$$\begin{aligned}
\boldsymbol{K}_{\mathrm{e}} &= \int_0^a \left[EI\bar{\boldsymbol{N}}_\chi^{\mathrm{T}}\bar{\boldsymbol{N}}_\chi + \kappa GA\left(\bar{\boldsymbol{N}}_\chi^{\mathrm{T}} - \bar{\boldsymbol{N}}\right)\left(\boldsymbol{N}_\chi - \bar{\boldsymbol{N}}\right) - m_{\mathrm{oil}} v_{\mathrm{oil}}^2 \boldsymbol{N}_\chi^{\mathrm{T}}\boldsymbol{N}_\chi\right]\mathrm{d}\,\chi \\
\boldsymbol{M}_{\mathrm{e}} &= \int_0^a \left[\left(m_{\mathrm{pipe}} + m_{\mathrm{oil}} + m_{\mathrm{water}}\right)\boldsymbol{N}^{\mathrm{T}}\boldsymbol{N} + (\rho I + \rho_{\mathrm{oil}} I_{\mathrm{oil}})\bar{\boldsymbol{N}}^{\mathrm{T}}\bar{\boldsymbol{N}}\right]\mathrm{d}\,\chi \\
\boldsymbol{C}_{\mathrm{e1}} &= \int_0^a \left(\boldsymbol{N}^{\mathrm{T}}\boldsymbol{N}_\chi - \boldsymbol{N}_\chi^{\mathrm{T}}\boldsymbol{N}\right)\mathrm{d}\,\chi
\end{aligned} \tag{9}$$

200

201 in which $\boldsymbol{N}_\chi = \partial\boldsymbol{N}/\partial\chi$ and $\bar{\boldsymbol{N}}_\chi = \partial\bar{\boldsymbol{N}}/\partial\chi$, superscript "T" denotes transposition, $\boldsymbol{K}_{\mathrm{e}}$

202 and $\boldsymbol{M}_{\mathrm{e}}$ are element stiffness and mass matrices, respectively. $\boldsymbol{C}_{\mathrm{e1}}$ is the gyroscopic

damping matrix due to the conveyed oil. Rayleigh damping is also considered here, and hence the element damping matrix can be expressed as

$$\boldsymbol{C}_{\mathrm{e}} = \boldsymbol{C}_{\mathrm{e1}} + d_1\boldsymbol{M}_{\mathrm{e}} + d_2\boldsymbol{K}_{\mathrm{e}} \tag{10}$$

where d_1 and d_2 are Rayleigh damping factors corresponding to the mass and stiffness, respectively.

The subsea pipeline is discretized into N Timoshenko beam elements, while the seabed is discretized into $N-2$ spring elements, as shown in Fig. 2. The discrete governing equation of the subsea pipeline can be written as

$$\boldsymbol{M}\ddot{\boldsymbol{X}} + \boldsymbol{C}\dot{\boldsymbol{X}} + \boldsymbol{K}\boldsymbol{X} = \boldsymbol{F}_{\mathrm{seabed}} \tag{11}$$

in which $\boldsymbol{M}$, $\boldsymbol{C}$ and $\boldsymbol{K}$ are structural mass, damping and stiffness matrices, respectively; $\boldsymbol{X}$ is the nodal displacement vector, $\boldsymbol{F}_{\mathrm{seabed}}$ is the reaction force vector of the seabed; and $\dot{}$ denotes differentiation with respect to time t.

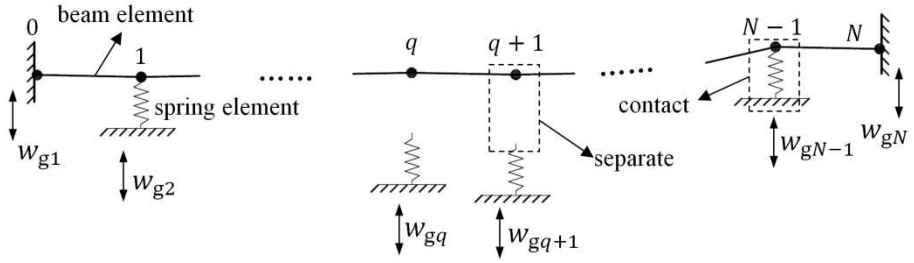

Fig. 2 Finite element model of subsea pipeline and seabed

Since the variation of earthquakes is considered, motions of different points at seabed will have differences in phases, amplitudes, or both. This means that the analysis of the subsea pipeline subjected to earthquake is a multi-support excitation problem. To solve this problem, Eq. (11) is rearranged as

$$\begin{bmatrix} \boldsymbol{M}_{\mathrm{s}} & \boldsymbol{M}_{\mathrm{sb}} \\ \boldsymbol{M}_{\mathrm{sb}}^{\mathrm{T}} & \boldsymbol{M}_{\mathrm{b}} \end{bmatrix} \begin{Bmatrix} \ddot{\boldsymbol{X}}_{\mathrm{s}} \\ \ddot{\boldsymbol{X}}_{\mathrm{b}} \end{Bmatrix} + \begin{bmatrix} \boldsymbol{C}_{\mathrm{s}} & \boldsymbol{C}_{\mathrm{sb}} \\ \boldsymbol{C}_{\mathrm{sb}}^{\mathrm{T}} & \boldsymbol{C}_{\mathrm{b}} \end{bmatrix} \begin{Bmatrix} \dot{\boldsymbol{X}}_{\mathrm{s}} \\ \dot{\boldsymbol{X}}_{\mathrm{b}} \end{Bmatrix} + \begin{bmatrix} \boldsymbol{K}_{\mathrm{s}} & \boldsymbol{K}_{\mathrm{sb}} \\ \boldsymbol{K}_{\mathrm{sb}}^{\mathrm{T}} & \boldsymbol{K}_{\mathrm{b}} \end{bmatrix} \begin{Bmatrix} \boldsymbol{X}_{\mathrm{s}} \\ \boldsymbol{X}_{\mathrm{b}} \end{Bmatrix} = \begin{Bmatrix} \boldsymbol{R}_{\mathrm{s}} \\ \boldsymbol{R}_{\mathrm{b}} \end{Bmatrix} \tag{12}$$

in which the subscripts “b” and “s” indicate the support and non-support degrees of freedom (DOF), respectively, so that $\boldsymbol{X}_{\mathrm{b}}$ are the enforced displacements of the supports on both sides, $\boldsymbol{X}_{\mathrm{s}}$ are all nodal displacements except those at the supports, $\boldsymbol{R}_{\mathrm{b}}$ are the enforced forces at the supports and $\boldsymbol{R}_{\mathrm{s}}$ are the reaction forces of the seabed. Expanding the first row of Eq. (12) gives

$$\boldsymbol{M}_{\mathrm{s}}\ddot{\boldsymbol{X}}_{\mathrm{s}} + \boldsymbol{C}_{\mathrm{s}}\dot{\boldsymbol{X}}_{\mathrm{s}} + \boldsymbol{K}_{\mathrm{s}}\boldsymbol{X}_{\mathrm{s}} = \boldsymbol{R}_{\mathrm{s}} + \boldsymbol{P} \tag{13}$$

in which $\boldsymbol{P} = -\boldsymbol{M}_{\mathrm{sb}}\ddot{\boldsymbol{X}}_{\mathrm{b}} - \boldsymbol{C}_{\mathrm{sb}}\dot{\boldsymbol{X}}_{\mathrm{b}} - \boldsymbol{K}_{\mathrm{sb}}\boldsymbol{X}_{\mathrm{b}}$ is the effective earthquake force acting on the non-support DOF.

Each node of the beam element used in this paper has two DOF, namely translation and rotation in the vertical plane. However, the reaction force of the seabed is assumed to act only on the translation DOF and not the rotation DOF of the pipeline during the contact. Combining Eqs. (2) and (3), the reaction force $\boldsymbol{R}_{\mathrm{s}}$ can be expressed as

$$
\begin{aligned}
&\boldsymbol{R}_{\mathrm{s}} = \mathbb{D}\boldsymbol{R} \\
&\boldsymbol{R}_q = \begin{cases} 0 & \xi_q > 0 \\ -K_{\mathrm{seabed}}\boldsymbol{\eta}_q & \xi_q = 0 \end{cases} \\
&\boldsymbol{\xi}_q = \boldsymbol{w}_q - \boldsymbol{\eta}_q - \boldsymbol{w}_{\mathrm{g}q}^{(0)} - \boldsymbol{w}_{\mathrm{g}q} \\
&q = 1,2,\cdots,N-1
\end{aligned} \tag{14}
$$

where $\boldsymbol{R}$ is the N_{ns}-dimensional reaction force vector and N_{ns} is the number of non-support nodes, $\mathbb{D}$ is the translation DOF indicator matrix with "0" and "1" elements, $\boldsymbol{\xi}$ is the relative displacement vector between the pipeline and seabed model, $\boldsymbol{w}$ is the translation vector of the pipeline, K_{seabed} is the stiffness of the seabed spring, $\boldsymbol{\eta}$ is the compressional deformation vector of the seabed, $\boldsymbol{w}_{\mathrm{g}}^{(0)}$ and $\boldsymbol{w}_{\mathrm{g}}$ are respectively the profile vector and displacement vector of the seabed.

2.3 Reduced computational model

Due to the contact nonlinearity, many iterations must be performed during the solution of Eq. (13). Meanwhile, the finite element model may have a large dimension and the dynamical analysis will be time consuming. In order to reduce the computational cost, one can project the nonlinear equations onto a relative lower dimensional subspace spanned by a set of specific basis functions and then the dimension of equations can be reduced [29]. In this paper, the basis used for reduction is the natural modes of the pipeline (without the seabed). The natural modes are obtained from the following generalized eigenvalue problem

$$
\boldsymbol{K}_{\mathrm{s}}\boldsymbol{\Phi}_p = \omega_p^2 \boldsymbol{M}_s \boldsymbol{\Phi}_p, \qquad p = 1,2,\cdots N_{\mathrm{mode}} \tag{15}
$$

in which ω_p and $\boldsymbol{\Phi}_p$ are the p-th natural frequency and mode of the system, respectively, N_{mode} is the dimension of $\boldsymbol{K}_{\text{s}}$ and $\boldsymbol{M}_{\text{s}}$. Thus, the reduced problem can be expressed as

$$\boldsymbol{X}_{\text{s}} = \boldsymbol{\Phi}\boldsymbol{q} \tag{16a}$$

$$\boldsymbol{M}_{\text{r}}\ddot{\boldsymbol{q}} + \boldsymbol{C}_{\text{r}}\dot{\boldsymbol{q}} + \boldsymbol{K}_{\text{r}}\boldsymbol{q} = \boldsymbol{r} + \boldsymbol{p} \tag{16b}$$

where

$$\begin{aligned} &\boldsymbol{\Phi} = [\boldsymbol{\Phi}_1 \quad \boldsymbol{\Phi}_2 \quad \cdots \quad \boldsymbol{\Phi}_n](n < N_{\text{mode}}) \\ &\boldsymbol{M}_{\text{r}} = \boldsymbol{\Phi}^{\text{T}}\boldsymbol{M}_{\text{s}}\boldsymbol{\Phi}, \qquad \boldsymbol{C}_{\text{r}} = \boldsymbol{\Phi}^{\text{T}}\boldsymbol{C}_{\text{s}}\boldsymbol{\Phi}, \qquad \boldsymbol{K}_{\text{r}} = \boldsymbol{\Phi}^{\text{T}}\boldsymbol{K}_{\text{s}}\boldsymbol{\Phi} \\ &\boldsymbol{r} = \boldsymbol{\Phi}^{\text{T}}\boldsymbol{R}_{\text{s}}, \qquad \boldsymbol{p} = \boldsymbol{\Phi}^{\text{T}}\boldsymbol{P} \end{aligned} \tag{17}$$

It is noted that Eq. (16b) cannot be decoupled into a set of single DOF systems for two reasons. Firstly, $\boldsymbol{C}_{\text{s}}$ contains the component of gyroscopic damping, which cannot be diagonalized by the natural modes. Secondly, $\boldsymbol{R}_{\text{s}}$ is not known a priori and depends on the current state of the pipeline and seabed due to the contact nonlinearity. This is different from the linear case or the case without internal oil.

3 Uncertain modelling of the earthquake and the pipeline

Two different kinds of uncertainties are considered in the present computational model. The first one is randomness of the earthquake and is modelled as a random process. The other one is modelling uncertainties of the pipeline, for which the random matrix theory is applied to model them.

3.1 Random earthquake with spatial variation

Assuming that the acceleration of the ground motion during the earthquake is a nonstationary random process, it can be expressed as

$$\ddot{w}_{\mathrm{g}} = g(t)\ddot{d}(t) \tag{18}$$

in which $\ddot{d}(t)$ is a stationary and homogeneous Gaussian random process with zero mean value and its auto power spectral density (PSD) is $S_0(\omega)$, ω is the circular frequency, $g(t)$ is a slowly varying deterministic envelope function. Then the cross-PSD of the acceleration at two arbitrary points can be expressed as

$$S\,(\Delta x, \omega) = \gamma(\Delta x, \omega) S_0(\omega) \tag{19}$$

where $\Delta x = \left|x_i - x_j\right|$ is the distance between the two points x_i and x_j on the ground, and $\gamma(\Delta x, \omega)$ is the coherency function which represents the spatial variation of earthquakes.

Considering n separate points on the ground, the auto-PSD matrix of the ground acceleration at these points has the form

$$\mathbf{S}(\omega) = \begin{bmatrix} \gamma_{11}(\omega) & \gamma_{12}(\omega) & \cdots & \gamma_{1n}(\omega) \\ \gamma_{21}(\omega) & \gamma_{22}(\omega) & \cdots & \gamma_{2n}(\omega) \\ \vdots & \vdots & \ddots & \vdots \\ \gamma_{n1}(\omega) & \gamma_{nn}(\omega) & \cdots & \gamma_{nn}(\omega) \end{bmatrix} S_0(\omega) \tag{20}$$

where $\gamma_{ij}(\omega)(i, j = 1,2, \cdots n)$ is the coherency function of x_i and x_j. By using

297 Cholesky decomposition, $\mathbf{S}(\omega)$ can be represented as the product of a lower triangular
298 matrix $\mathbf{H}(\omega)$ and its Hermitian transpose, i.e.
299

$$\mathbf{S}(\omega) = \mathbf{H}(\omega)\mathbf{H}^{\mathrm{H}}(\omega) \tag{21}$$

300
301 The stationary time history sample of the acceleration at point x_i is obtained in the
302 following terms as a summation of cosine functions with random phase angles [30]
303

$$\ddot{d}_i(t) = 2\sum_{l=1}^{i}\sum_{m=1}^{N_{\mathrm{freq}}} |H_{il}(\omega_m)|\sqrt{\Delta\omega}\cos(\omega_m t - \theta_{il}(\omega_m) + \Phi_{lm}) \tag{22}$$

304
305 where $H_{il}(\omega_m)$ is the element on the i-th row and l-th column of matrix $\mathbf{H}(\omega_m)$,
306 $\Delta\omega = \omega_{\mathrm{cut}}/N$ is the frequency step, ω_{cut} is the cut off frequency, N is the number of
307 frequency steps, N_{freq} is the number of frequencies, $\omega_m = m\Delta\omega$ is the m-th
308 frequency, $\theta_{il}(\omega_m)$ is the phase of $H_{il}(\omega_m)$, and Φ_{lm} is the random phase angle
309 distributed uniformly between 0 and 2π. The corresponding nonstationary time history
310 sample can then be obtained according to Eq. (18). The reader is referred to [31] for a
311 more detailed illustration of the simulation procedure of random earthquakes with spatial
312 variations.

313 3.2 Nonparametric modelling for uncertainties of the pipeline

314 As mentioned in the introduction, the nonparametric approach developed by Soize
315 [6] is able to take into account modelling uncertainties in the computational model. This
316 subsection will show the main theories and derivations of the nonparametric approach

and more details can be found in [6, 7].

The uncertainties of mass, damping and stiffness matrices are considered and these matrices are replaced by the corresponding random matrices. Thus the governing equations shown in Eq. (16b) can be rewritten as

$$\boldsymbol{M}_{\mathrm{r}}^{\mathrm{npar}}\ddot{\boldsymbol{q}}+\boldsymbol{C}_{\mathrm{r}}^{\mathrm{npar}}\dot{\boldsymbol{q}}+\boldsymbol{K}_{\mathrm{r}}^{\mathrm{npar}}\boldsymbol{q}=\boldsymbol{r}+\boldsymbol{p} \tag{23}$$

where $\boldsymbol{M}_{\mathrm{r}}^{\mathrm{npar}}$, $\boldsymbol{C}_{\mathrm{r}}^{\mathrm{npar}}$, $\boldsymbol{K}_{\mathrm{r}}^{\mathrm{npar}}$ are $n\times n$ symmetric positive-definite random matrices corresponding to the mass, damping and stiffness, respectively.

According to the random matrix theory [6], $p_{\boldsymbol{A}}$, the probability density function of the random matrix $\boldsymbol{A}\left(\boldsymbol{A}\in\boldsymbol{M}_{\mathrm{r}}^{\mathrm{npar}},\boldsymbol{C}_{\mathrm{r}}^{\mathrm{npar}},\boldsymbol{K}_{\mathrm{r}}^{\mathrm{npar}}\right)$, yields the following constraint conditions

$$\begin{cases}\displaystyle\int_{\mathbb{M}_n^+(\mathbb{R})} p_{\boldsymbol{A}}(\boldsymbol{A})\tilde{\mathrm{d}}\boldsymbol{A}=1\\ \displaystyle\int_{\mathbb{M}_n^+(\mathbb{R})} \boldsymbol{A}p_{\boldsymbol{A}}(\boldsymbol{A})\tilde{\mathrm{d}}\boldsymbol{A}=\underline{\boldsymbol{A}}\in\mathbb{M}_n^+(\mathbb{R})\\ \displaystyle\int_{\mathbb{M}_n^+(\mathbb{R})} \ln\left(\det(\boldsymbol{A})\right)p_{\boldsymbol{A}}(\boldsymbol{A})\tilde{\mathrm{d}}\boldsymbol{A}=v\ \text{ with }|v|<+\infty\end{cases} \tag{24}$$

where $\mathbb{M}_n^+(\mathbb{R})$ indicates the subspace constituted of all the positive-definite symmetric real matrices with $n\times n$ dimensions, $\tilde{\mathrm{d}}\boldsymbol{A}=2^{n(n-1)/4}\prod_{1\le i\le j\le n}\mathrm{d}\boldsymbol{A}_{ij}$ and $\underline{\boldsymbol{A}}$ is the mean value of the random matrix $\boldsymbol{A}$. Taking into account the constraint conditions in Eq. (24) and using the Maximum Entropy Principle, the probability density function of $\boldsymbol{A}$ can be deduced as

335

$$p_{\boldsymbol{A}}(\boldsymbol{A}) = \mathbb{I}_{\mathbb{M}_n^+(\mathbb{R})}(\boldsymbol{A}) \times c_{\boldsymbol{A}} \times \left(\det(\boldsymbol{A})\right)^{\lambda-1} \times \exp\left(-\frac{(n-1+2\lambda)}{2}\mathrm{tr}\{\underline{\boldsymbol{A}}^{-1}\boldsymbol{A}^{\mathrm{T}}\}\right) \quad (25)$$

336

337 where $\mathbb{I}_{\mathbb{M}_n^+(\mathbb{R})}(\boldsymbol{A})$ is the indicator function, which is equal to 1 when $\boldsymbol{A} \in \mathbb{M}_n^+(\mathbb{R})$ and

338 0 otherwise, $c_{\boldsymbol{A}}$ is a positive constant which can be expressed as

339

$$c_{\boldsymbol{A}} = \frac{(2\pi)^{-n(n-1)/4}\left(\frac{n-1+2\lambda}{2}\right)^{n(n-1+2\lambda)/2}}{\left\{\prod_{l=1}^{n}\Gamma\left(\frac{n-l+2\lambda}{2}\right)\right\}\left(\det(\underline{\boldsymbol{A}})\right)^{(n-1+2\lambda)/2}} \quad (26)$$

340

341 where $\Gamma(x) = \int_0^{+\infty} t^{x-1}\mathrm{e}^{-t}\,\mathrm{d}t (x > 0)$ is the gamma function.

342 The variance of the component $\boldsymbol{A}_{jk}$ which is at the j-th row and k-th column of

343 matrix $\boldsymbol{A}$ can be calculated from

344

$$\sigma_{jk} = \frac{1}{n-1+2\lambda}\left(\underline{\boldsymbol{A}}_{jk}^2 + \underline{\boldsymbol{A}}_{jj}\underline{\boldsymbol{A}}_{kk}\right), \qquad 0 < j \le k \le n \quad (27)$$

345

346 Note that $\mathrm{E}\left\{\left\|\boldsymbol{A} - \underline{\boldsymbol{A}}\right\|_{\mathrm{F}}^2\right\} = \sum_j \sum_k \sigma_{jk}^2$, in which $\|\boldsymbol{A}\|_{\mathrm{F}}^2 = \left(\mathrm{tr}(\boldsymbol{A}\boldsymbol{A}^*)\right)^{1/2}$ is the Frobenius

347 norm of the matrix $\boldsymbol{A}$, $\boldsymbol{A}^*$ is the conjugate of the matrix $\boldsymbol{A}$ and tr( ) denotes the trace.

348 Thus the dispersion parameter of the matrix $\boldsymbol{A}$ can be defined as

349

$$\delta_{\boldsymbol{A}} = \left\{\frac{\mathrm{E}\left\{\left\|\boldsymbol{A} - \underline{\boldsymbol{A}}\right\|_{\mathrm{F}}^2\right\}}{\left\|\underline{\boldsymbol{A}}\right\|_{\mathrm{F}}^2}\right\}^{\frac{1}{2}} = \left\{\frac{1}{n-1+2\lambda}\left(1 + \frac{\left(\mathrm{tr}(\underline{\boldsymbol{A}})\right)^2}{\left(\mathrm{tr}(\underline{\boldsymbol{A}}^2)\right)}\right)\right\}^{\frac{1}{2}} \quad (28)$$

350

351 Then the parameter λ in Eqs. (25) to (28) can be calculated by

352

$$\lambda = \frac{1}{2\delta_A^2}\left(1 - \delta_A^2(n-1) + \frac{\left(\mathrm{tr}(\underline{\boldsymbol{A}})\right)^2}{\left(\mathrm{tr}(\underline{\boldsymbol{A}}^2)\right)}\right) \tag{29}$$

353

354 From the above derivation, it can be seen that once the dimension n has been

355 determined, $\delta_{\boldsymbol{A}}$ controls the dispersion level of the random matrix $\boldsymbol{A}$ and hence is called

356 the "dispersion parameter". It is proved that $\delta_{\boldsymbol{A}}$ should satisfy the following constraint

357

$$0 < \delta_{\boldsymbol{A}} < \sqrt{\frac{n+1}{n+5}} \tag{30}$$

358

359 Given a dispersion parameter $\delta_{\boldsymbol{A}}$ and mean value matrix $\underline{\boldsymbol{A}}$, samples of the random

360 matrix $\boldsymbol{A}$ can then be generated. Since $\boldsymbol{A}$ is a positive-definite symmetric matrix, it can

361 be written as

362

$$\boldsymbol{A} = \underline{\boldsymbol{L}}_{\boldsymbol{A}}^{\mathrm{T}} \boldsymbol{G} \underline{\boldsymbol{L}}_{\boldsymbol{A}} \tag{31}$$

363

364 in which, $\underline{\boldsymbol{L}}_{\boldsymbol{A}}$ is an upper triangular matrix obtained by applying the Cholesky

365 factorization to $\underline{\boldsymbol{A}}$, i.e., $\underline{\boldsymbol{A}} = \underline{\boldsymbol{L}}_{\boldsymbol{A}}^{\mathrm{T}} \underline{\boldsymbol{L}}_{\boldsymbol{A}}$, $\boldsymbol{G}$ is a random matrix and whose mean value is a n-

366 dimensional identity matrix. The random matrix $\boldsymbol{G}$ is further written as

367

$$\boldsymbol{G} = \boldsymbol{L}_{\boldsymbol{G}}^{\mathrm{T}} \boldsymbol{L}_{\boldsymbol{G}} \tag{32}$$

368

369 where $\boldsymbol{L}_{\boldsymbol{G}}$ is an upper triangular random matrix resulting from the Cholesky factorization

370 and its samples can be generated by the following steps [12]:

371 (1) random variables $\boldsymbol{L}_{jk}(j \leq k)$ are assumed to be independent;

(2) for a non-diagonal element, i.e. $j < k$, the real-valued random variable $\boldsymbol{L}_{\boldsymbol{G}jk}$ can be rewritten as $\boldsymbol{L}_{\boldsymbol{G}jk} = \sigma_n |U_{jk}|$, in which $\sigma_n = \delta_{\boldsymbol{A}}(n+1)^{-1/2}$ and U_{jk} is a Gaussian random variable with zero mean and variance of 1;

(3) for a diagonal element, i.e. $j = k$, the positive-valued random variable $\boldsymbol{L}_{\boldsymbol{G}jk}$ can be rewritten as $\boldsymbol{L}_{\boldsymbol{G}jj} = \sigma_n\sqrt{2V_j}$ in which σ_n is defined in step (2) and V_j is a gamma random variable with the following probability density function

$$p_{V_j}(v) = \mathbb{I}_{\mathbb{M}_n^+(\mathbb{R})}(v)\frac{1}{\Gamma(\alpha_{n,j})}v^{\alpha_{n,j}-1}\mathrm{e}^{-v}, \qquad \alpha_{n,j} = \frac{n+1}{2\delta_{\boldsymbol{A}}^2} + \frac{1-j}{2} \tag{33}$$

4 Numerical examples

The physical and geometric parameters of the subsea pipeline are taken as follows: Young's modulus $E = 207 \times 10^9\mathrm{Pa}$, mass density $\rho = 7850\,\mathrm{kg/m^3}$, Poisson's ratio $\nu = 0.3$, Rayleigh damping factors corresponding to the stiffness $d_1 = 0.05$ and the mass $d_2 = 0.01$, total length of pipeline $L_0 = 100\mathrm{m}$, shear correction factor $\kappa = 2(1+\nu)/(4+3\nu)$, outer radius $R_{\mathrm{out}} = 0.6\mathrm{m}$, wall thickness $h = 0.017\mathrm{m}$. The mass densities of the oil in the pipeline and surrounding water are $\rho_{\mathrm{oil}} = 800\,\mathrm{kg/m^3}$ and $\rho_{\mathrm{water}} = 1025\,\mathrm{kg/m}$, respectively, and the velocity of the oil is $v_{\mathrm{oil}} = 3\,\mathrm{m/s}$.

According to the design standard [32], the effective axial compression N_0 should not exceed $0.5N_{\mathrm{cr}}$, where N_{cr} is the critical buckling load, and hence $N_0 = 0.3N_{\mathrm{cr}}$ is used in this paper. The pipeline is discretized into 100 elements and both ends are simply supported.

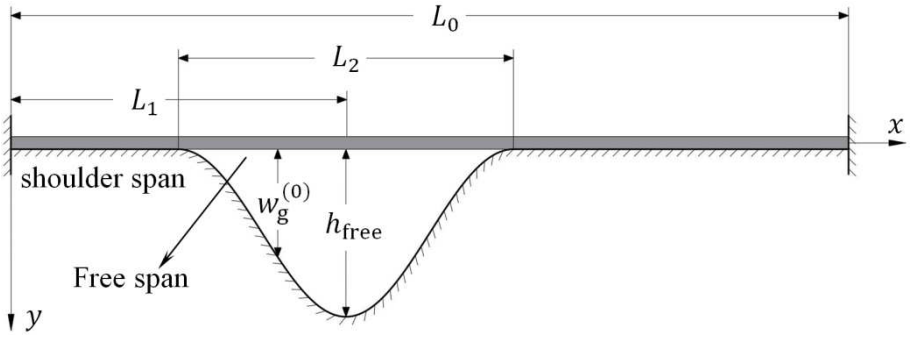

Fig. 3 Schematic of seabed profile

A seabed profile shown in Fig. 3 is considered. The middle point of the free span is $L_1 = 50\text{m}$, the length is $L_2 = 50\text{m}$, the maximum depth is $h_{\text{free}} = 0.3\text{m}$. The depth distribution of the free span is represented approximately by a cosine function, hence the seabed profile can be expressed as

$$w_{\text{g}}^{(0)} = \begin{cases} 0 & 0 \le x < L_1 - L_2/2 \\ \dfrac{h_{\text{free}}}{2}\left[1 - \cos\dfrac{2\pi(x - L_1 + L_2/2)}{L_2}\right] & L_1 - L_2/2 \le x < L_1 + L_2/2 \\ 0 & L_1 + L_2/2 \le x \le L_0 \end{cases} \quad (34)$$

A ground acceleration spectrum power density function developed by Clough and Penzien [33] is used here, and the corresponding parameters are $S_{\text{g}} = 0.018\,\text{m}^2/\text{s}^3$, $\omega_{\text{g}} = 15\,\text{rad/s}$, $\omega_{\text{f}} = 0.1\omega_{\text{g}}$, $v_{\text{app}} = 1000\,\text{m/s}$, $\xi_{\text{g}} = \xi_{\text{f}} = 0.6$ [34]. The duration of the earthquake is $T = 10.92\text{s}$, and the time step for the numerical integration is $\Delta t = 0.01\text{s}$, hence the number of time steps is $N_t = 1093$. The nonstationary modulation function and spatial variation parameters of earthquake can be found in [31]. Samples of ground acceleration are generated by Eqs. (18) and (22), and then a correction scheme suggested by Berg and Housner [35] is used to eliminate the baseline offsets caused by

408 the accumulation of random noise in accelerations.

409 In this section, the optimal numbers of reduced modes and MCS samples are firstly
410 determined through convergence analysis. Then, the propagations of randomness of the
411 earthquake and modelling uncertainties of the seabed are investigated. Since the unilateral
412 contact of the pipeline and seabed introduces nonlinearity into the computational model,
413 the randomness and modelling uncertainties may have some different influences on
414 random responses. Hence, a model of permanent contact between the pipeline and seabed
415 is also used for a comparative study. It is noted that in the permanent contact model, the
416 system stiffness matrix contains two components, namely, the pipeline and seabed.
417 However, to be consistent with the unilateral contact model, only the pipeline is assumed
418 to be uncertain while the seabed is assumed to be deterministic.

419 ## 4.1 Convergence analysis

420 The convergence problem of the number of reduced modes is studied based on the
421 mean model of the system, and the excitation is an arbitrary sample of the ground motions.
422 The study uses the following convergence function
423

$$\mathrm{Conv}(n_b) = \int_0^T \|\boldsymbol{w}(t, n_b)\|^2 \mathrm{d}t \tag{35}$$

424

425 in which $\boldsymbol{w}(t, n_b)$ is the displacement vector of the pipeline at time t by using the first
426 n_b natural modes as reduced modes. For the convenience of comparing the cases of
427 unilateral and permanent contact on a same figure, results are normalized by those with

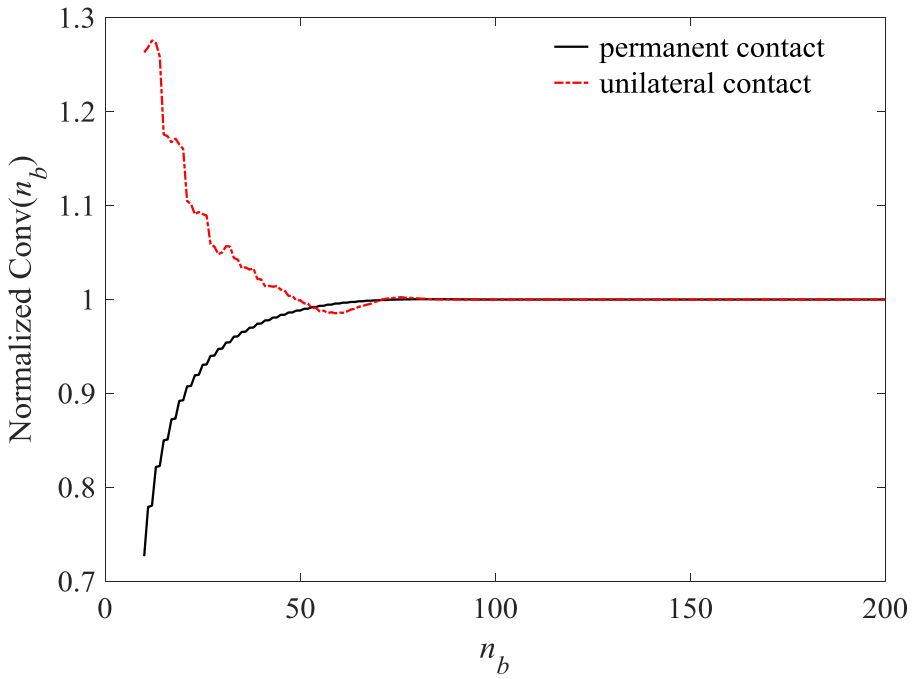

Fig. 4 Normalized convergence results for reduced modes in permanent and unilateral contact models

$n_b = 200$, which is the case without any reduction. Fig. 4 gives the convergence results, which indicate that both unilateral and permanent contact models will obtain convergent results when $n_b \geq 80$. Hence, $n_b = 80$ is used in the subsequent analysis.

On the other hand, since the random results are obtained by MCS, it is necessary to study the convergence of MCS samples. The corresponding convergence function can be defined as [36]

$$\mathrm{Conv}(n_s) = \frac{1}{n_s}\sum_{i=1}^{n_s}\int_0^T \|\boldsymbol{w}(t,s_i)\|^2 \mathrm{d}t \tag{31}$$

where $\boldsymbol{w}(t,s_i)$ indicates the displacement vector of the pipeline for the i-th sample at time t and n_s is the total number of samples. The convergence results for cases with

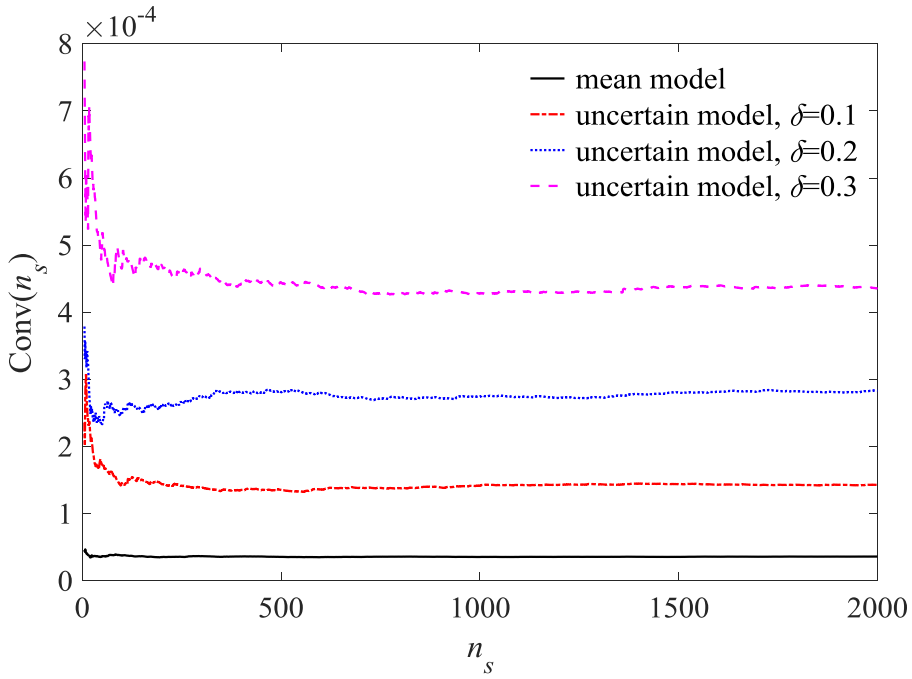

441

442 (a) Permanent contact model

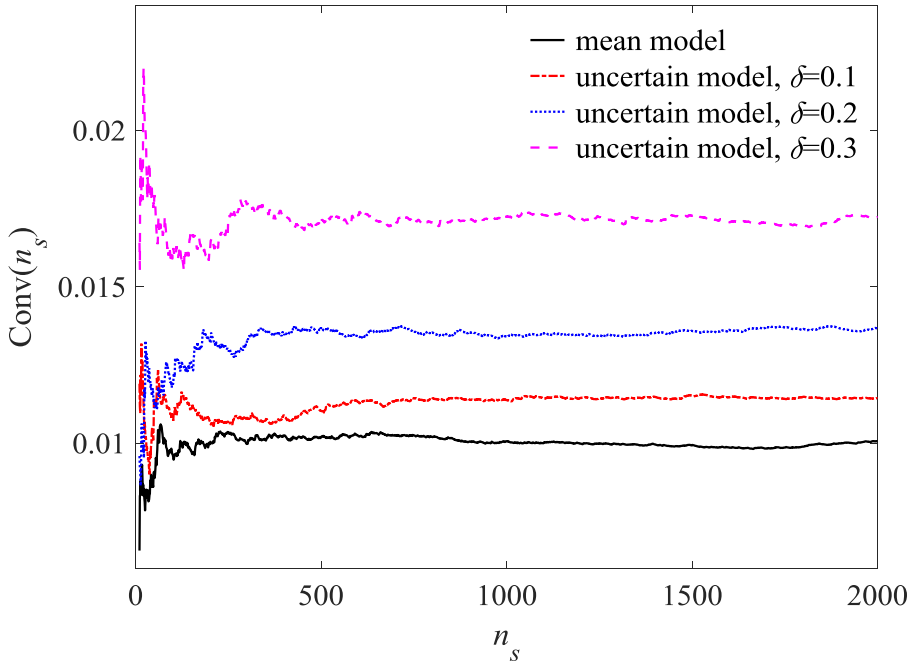

443

444 (b) Unilateral contact model

445 Fig. 5 Convergence results for numbers of Monte Carlo simulation in permanent and

446 unilateral contact models

447 different dispersion parameters, i.e., $\delta_M = \delta_K = 0.1,\ 0.2,\ 0.3$, are calculated and shown
448 in Fig. 5. It can be seen that the permanent contact model appears to have a faster
449 convergence with the number of samples than the unilateral contact model. To balance
450 the accuracy and efficiency, $n_s = 1000$ is used in following studies. It is worth noting
451 that the number of MCS samples is always chosen to be in the range of about 200 to 1500
452 in the relevant literature [6-14, 36].

453 4.2 Propagations of randomness and modelling uncertainties

454 In the present computational model, two kinds of uncertainty, namely, the
455 randomness of ground motions and modelling uncertainties of the pipeline are included.
456 To study the propagations of these uncertainties qualitatively, three representative cases
457 with different uncertainties are considered and their details are shown in Table 1.

458 Table. 1 Three representative cases with different uncertainties

	Ground motions	Pipeline
Case 1	Deterministic Arbitrary sample	Modelling uncertainties Random matrix
Case 2	Randomness Random process	Deterministic Mean model
Case 3	Randomness Random process	Modelling uncertainties Random matrix

4.2.1 Case 1: deterministic ground motions and uncertain pipeline model

To study the influences of modelling uncertainties on random responses, the case with deterministic ground motions and an uncertain pipeline model is carried out firstly. The ground motion is an arbitrary sample generated by the approach in subsection 3.1. Time histories of this sample at $x = 50\mathrm{m}$ are given in Fig. 6.

Fig. 7 displays the time-varying mean values of displacements of the pipeline at $x = 50\mathrm{m}$ for cases with different dispersion parameters. It is shown that the dispersion parameters of modelling uncertainties have slight influences on the mean values of responses in the permanent contact model. However these influences are very significant in the unilateral contact model, giving larger mean values as the dispersion parameters are increased. Fig. 8 gives the time-varying standard deviations of displacement responses at the same location. It can be seen that standard deviations increase with dispersion parameters in both the permanent and unilateral contact models. However, this increase is almost linear in the permanent contact model, while it is clearly nonlinear in the unilateral contact model. These results demonstrate that the modelling uncertainties of the pipeline have significantly different propagation in linear and nonlinear systems.

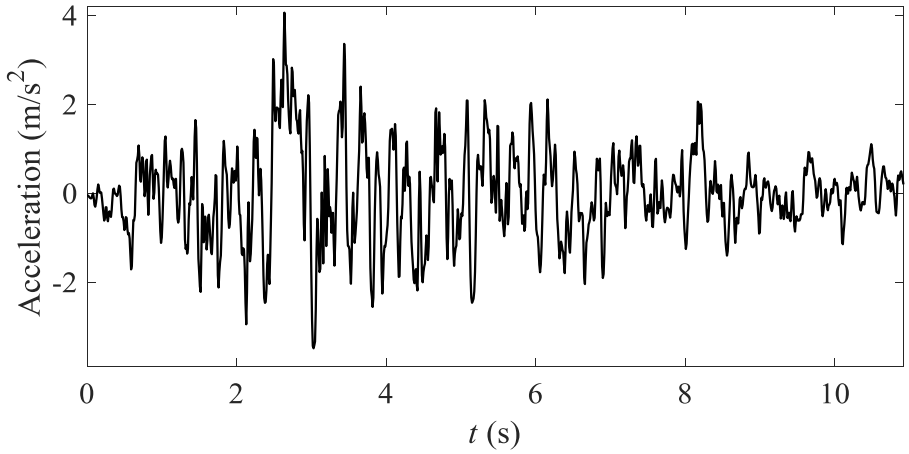

(a) Acceleration

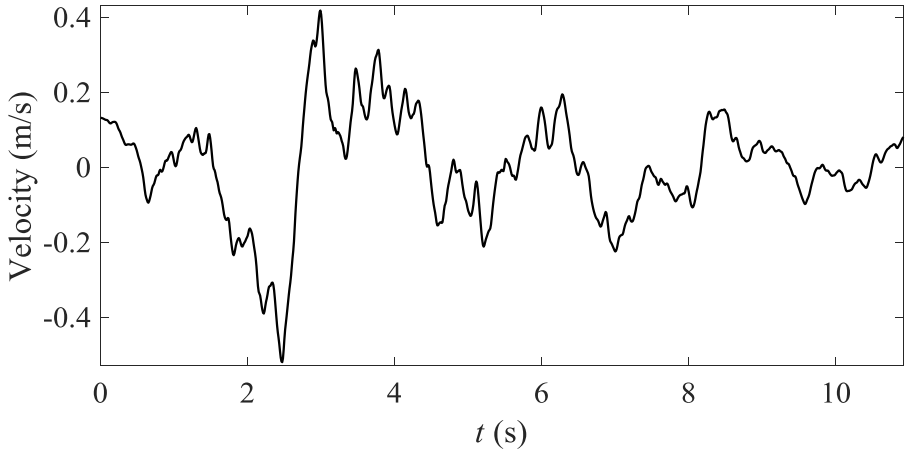

(b) Velocity

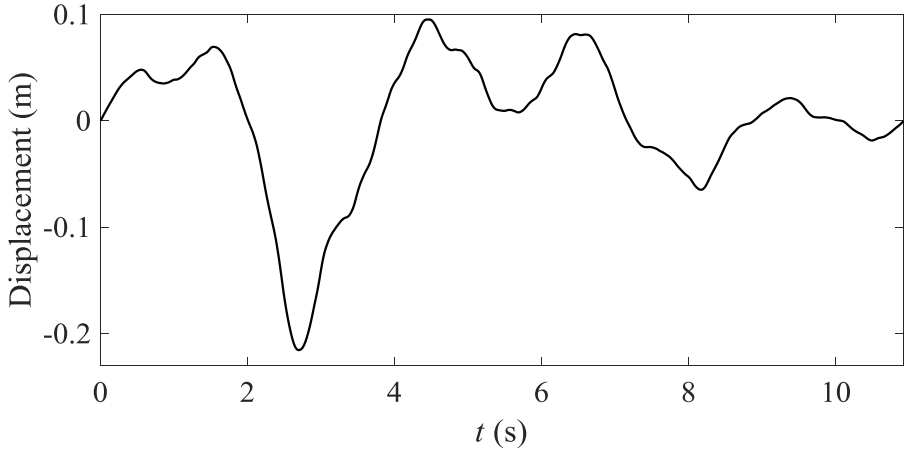

(c) Displacement

Fig. 6 Time histories of the ground motion at $x = 50$m

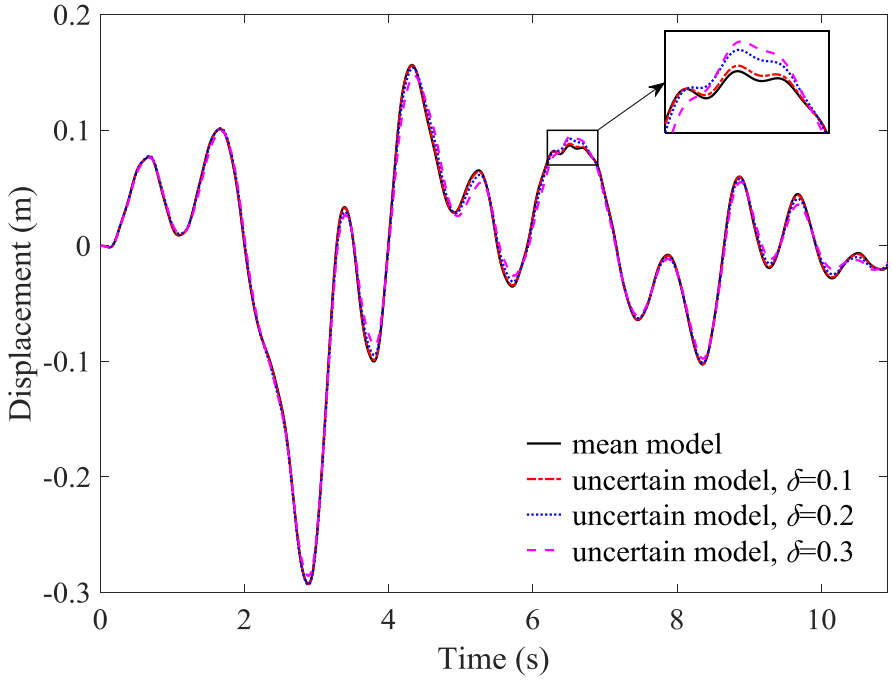

(a) Permanent contact model

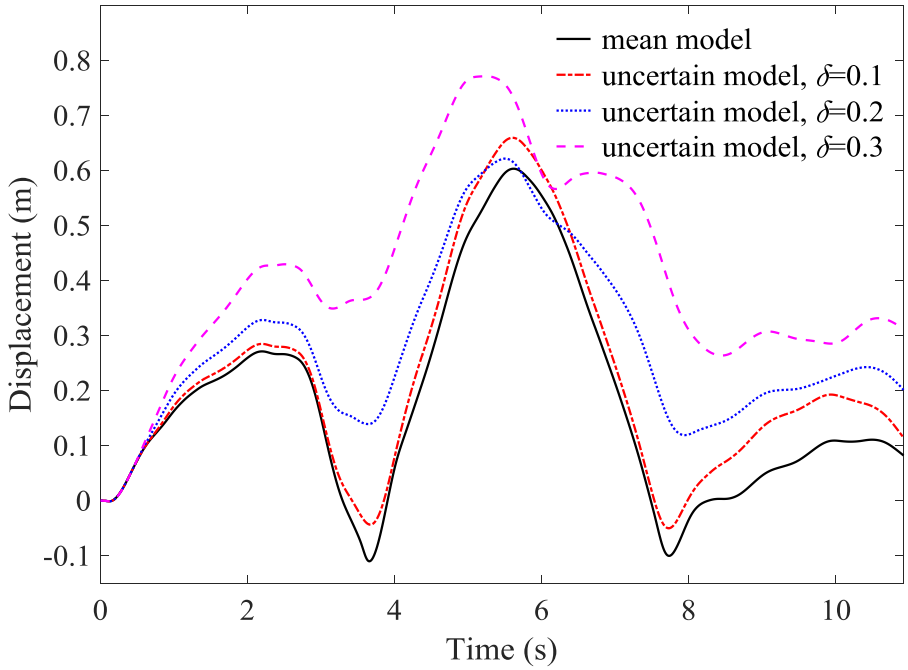

(b) Unilateral contact model

Fig. 7 Mean values of pipeline displacements for the case of deterministic ground motions and uncertain pipeline model

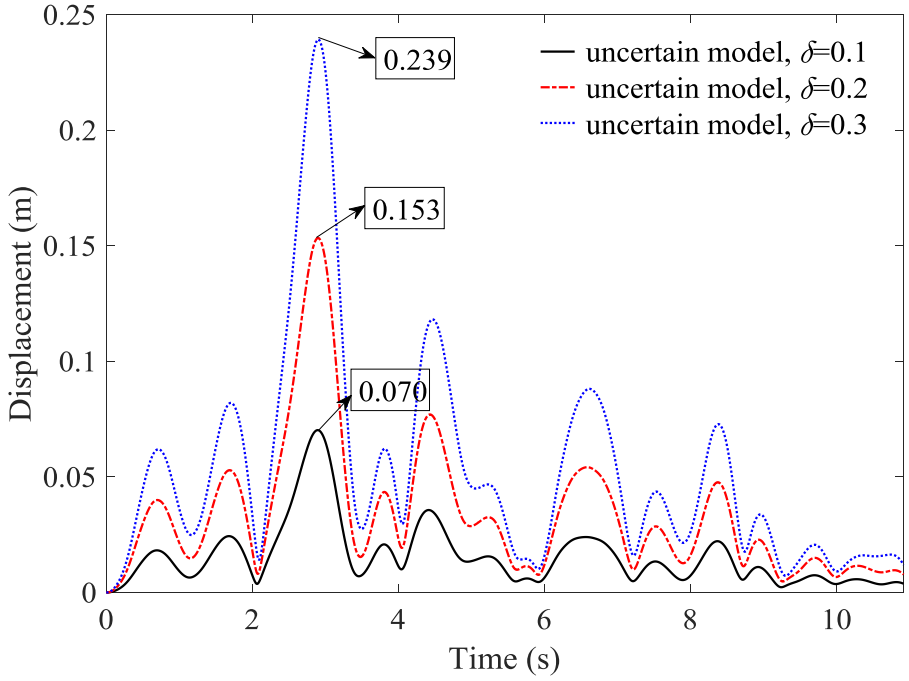

(a) Permanent contact model

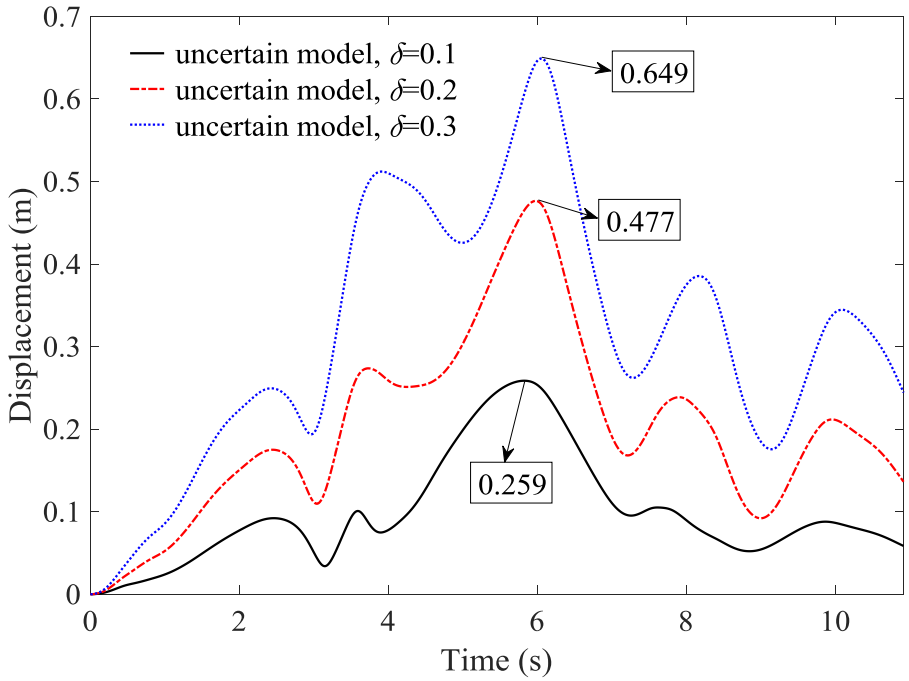

(b) Unilateral contact model

Fig. 8 Standard deviations of pipeline displacements for the case of deterministic ground motions and uncertain pipeline model

4.2.2 Case 2: random ground motions and deterministic pipeline

In this subsection, a computational model with random ground motions and deterministic pipeline model is adopted to study the propagation of randomness of the earthquake. Note that the ground motions are assumed to be Gaussian distributed with zero mean.

Fig. 9 presents the time-varying statistical moments of displacements of the pipeline at $x = 50\text{m}$ in the permanent and unilateral contact models. It can be seen from Fig. 9(a) that the responses have zero mean values in the permanent contact model while much larger mean values in the unilateral contact model. The reason is that for a linear and time-invariant system (the permanent contact model), if the input has zero mean, then the output also has zero mean. However, in the unilateral contact model which is a nonlinear

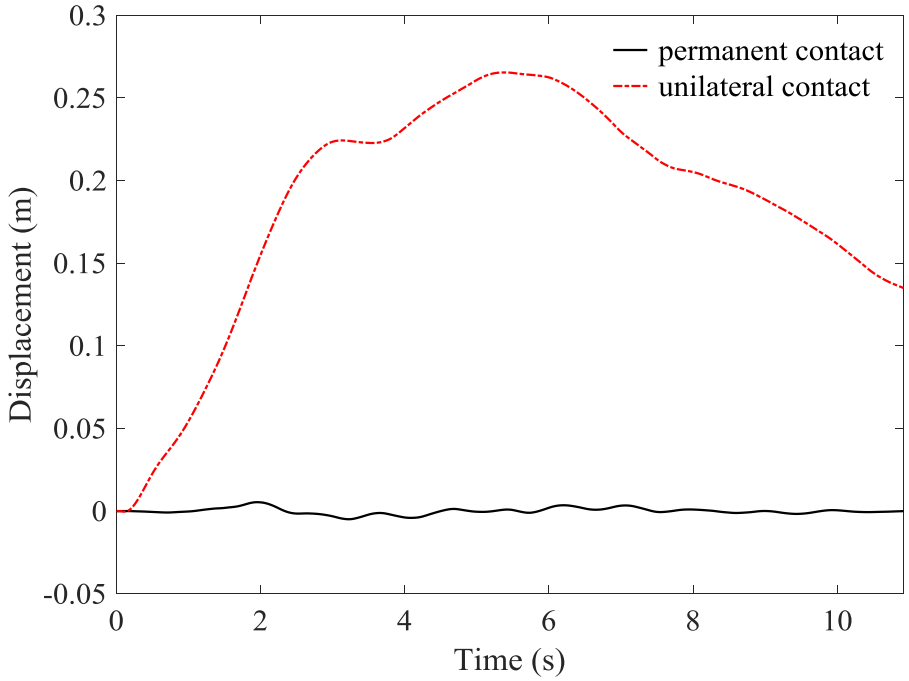

(a) Mean values

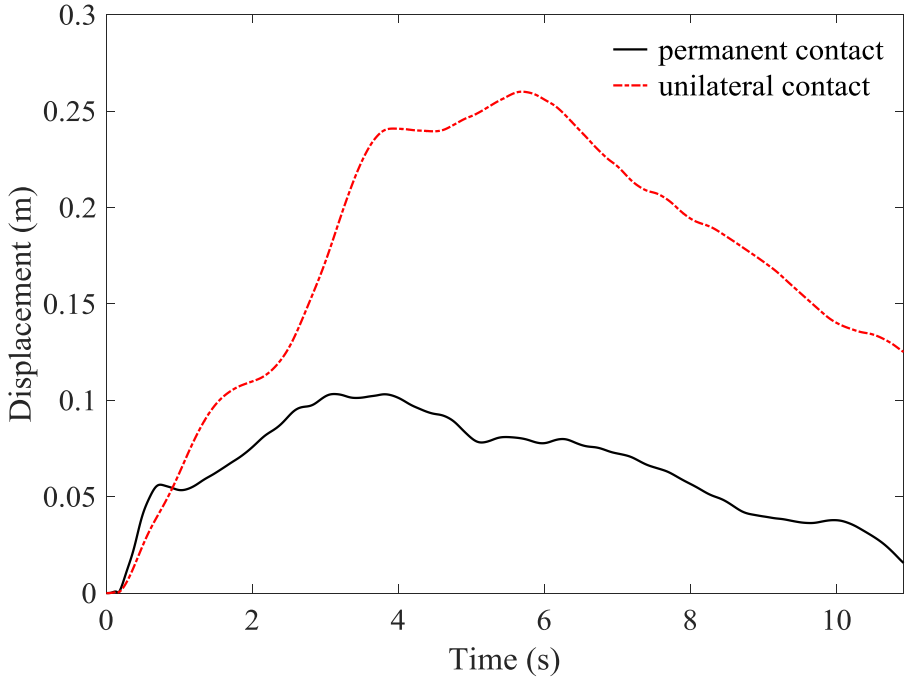

(b) Standard deviations

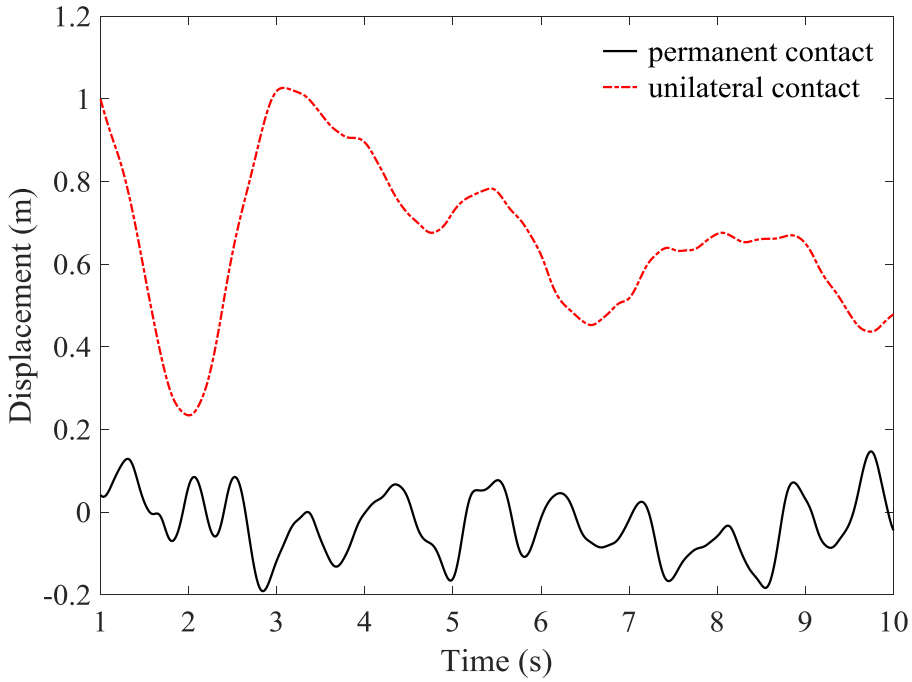

(c) Skewnesses

Fig. 9 Statistical moments of pipeline displacements for the case of random ground motions and deterministic pipeline model

system, the responses have non-zero mean values even if the excitation has zero mean values. Fig. 9(b) gives the standard deviations. It is observed that the standard deviations in the unilateral contact model are much larger than those in the permanent contact model, except for a short time at the beginning of the earthquake. The skewness, which is a measure of the asymmetry from the Gaussian distribution, is given in Fig. 9(c). It can be seen that both skewnesses fluctuate around zero, with a small amplitude in the permanent contact model but relatively large values in the unilateral contact model. This phenomenon indicates that when the ground motions are Gaussian, the responses of the permanent contact are also Gaussian while those of the unilateral contact models are not. Based on these results, it is concluded that the randomness of the ground motions propagates in different ways in the permanent and unilateral contact models.

4.2.3 Case 3: random ground motions and uncertain pipeline

Finally, a case with random ground motions and an uncertain pipeline model is carried out to study the combined influences of the randomness and modelling uncertainties on random responses. The time-varying mean values of displacements of the pipeline at $x = 50\text{m}$ are shown in Fig. 10. It can be seen that for the permanent contact model, the mean values vary in a small range around zero with amplitudes of the order 10^{-3}m, which means that random responses can be regarded as being zero mean. It is also shown that the influence of the dispersion parameter on the amplitude of mean values is not obvious in the permanent contact model. However, as shown in Fig. 10(b), the dispersion

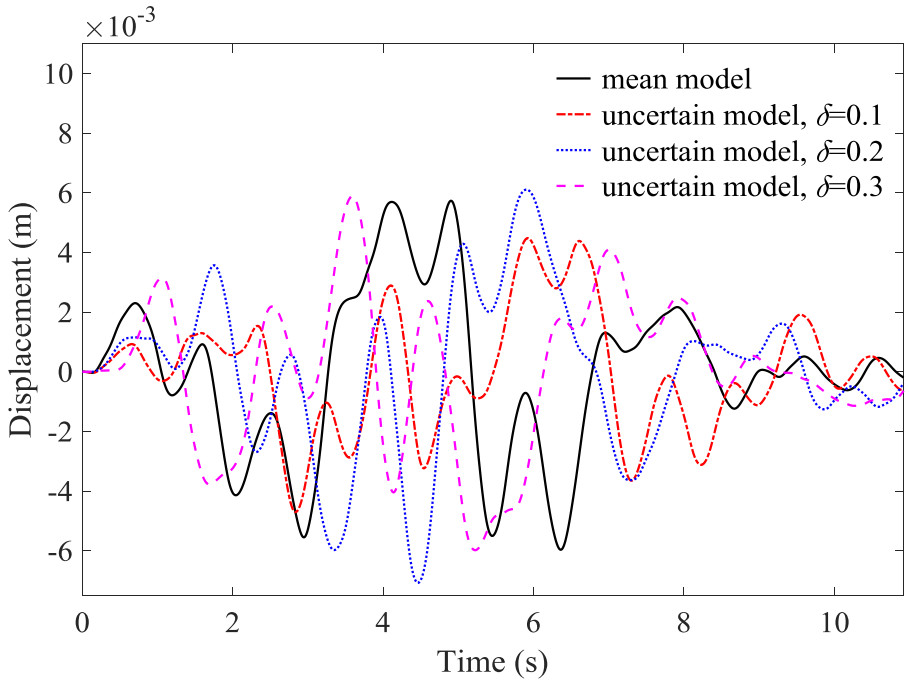

(a) Permanent contact model

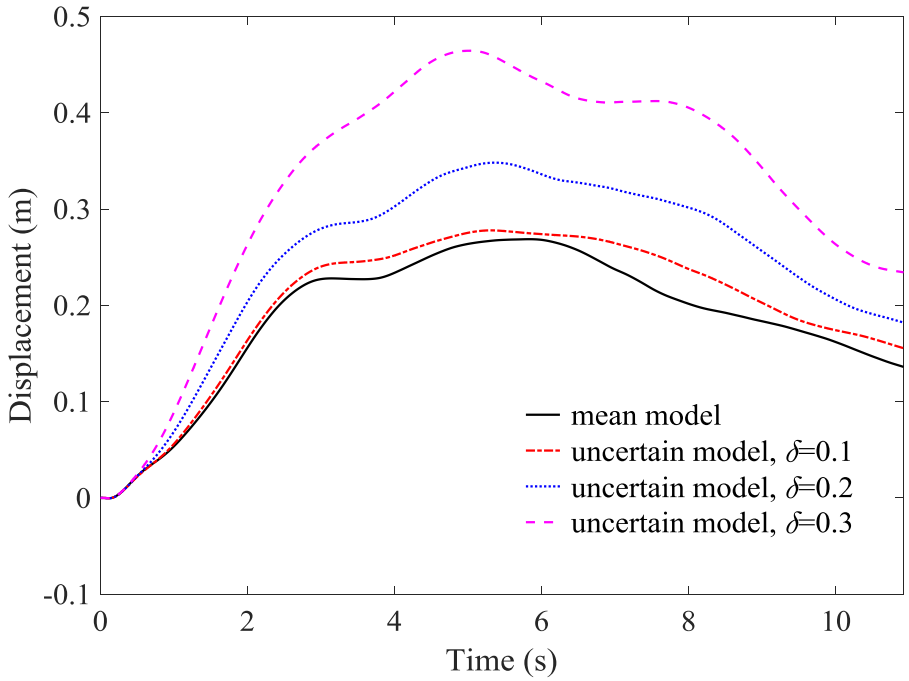

(b) Unilateral contact model

Fig. 10 Mean values of pipeline displacements for the case of random ground motions and uncertain pipeline model

543 parameter has a remarkable influence on the mean values for the unilateral contact model.
544 Fig. 11 shows the time-varying standard deviations of displacement responses and the
545 characteristics of results are quite similar to those in Fig. 8. However, the standard
546 deviations in Fig. 11 do not increase linearly with the dispersion parameter any more for
547 the permanent contact model, in contrast to those in Fig. 8. Compared to the results for
548 Cases 1 and 2, it can be concluded that the consideration of both randomness and
549 modelling uncertainty will make random responses more dispersed than the cases in
550 which either one is not considered.

551 The reliability assessment of structures subjected to an earthquake is usually
552 formulated as a first passage problem, i.e. the probability that the structural response
553 exceeds a given threshold. Based on certain assumptions, the first passage problem is
554 usually reduced to finding the statistical moments of the maximum response during a
555 specified period. Figs. 12 and 13 give mean values and standard deviations of maximum
556 displacement responses of the pipeline, respectively. It is shown that both mean values
557 and standard deviations tend to increase with the dispersion parameter, especially those
558 in the middle region of the pipeline. Meanwhile, it can be seen that mean values and
559 standard deviations near the end supports, i.e., locations $x = 0$ to 20m and $x = 80$ to
560 100m, vary little with the increase of the dispersion parameter in the permanent contact
561 model (Figs. 12(a) and 13(a)), but vary greatly for the unilateral contact model (Figs. 12(b)
562 and 13(b)). There are two reasons for this phenomenon. Firstly, the end supports of the

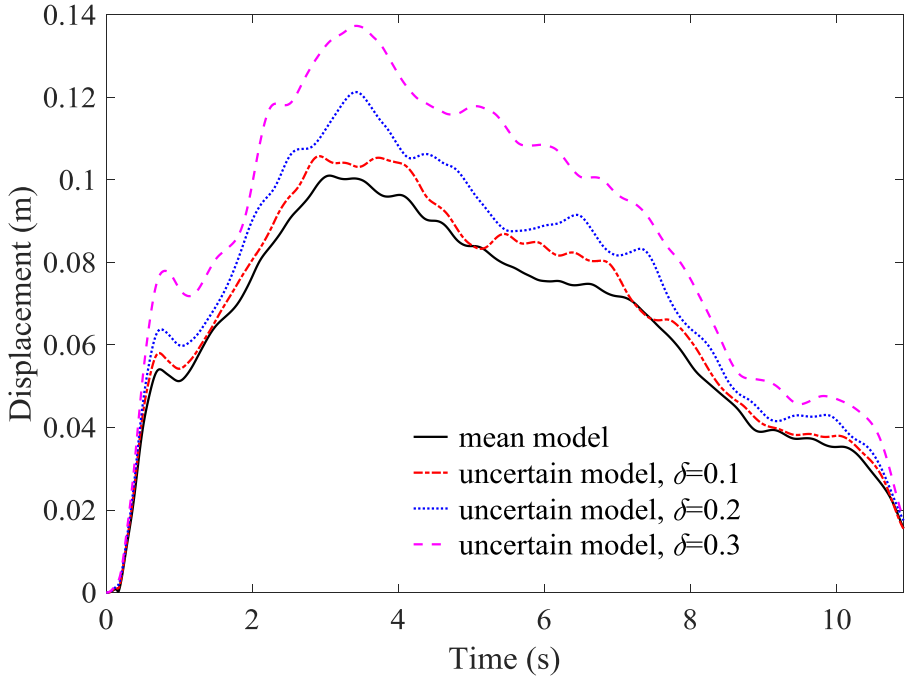

(a) Permanent contact model

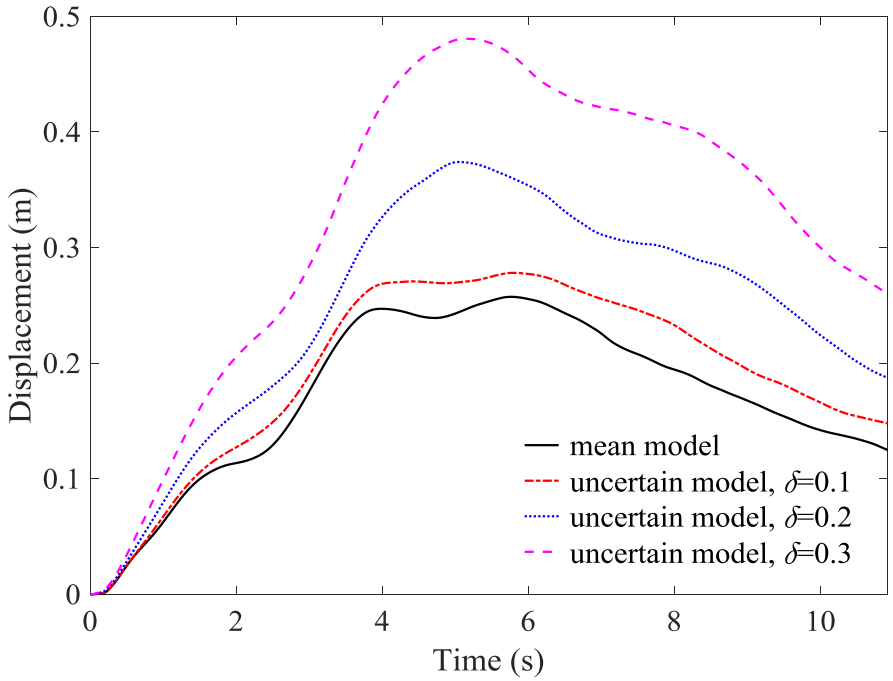

(b) Unilateral contact model

Fig. 11 Standard deviations of pipeline displacements for the case of random ground motions and uncertain pipeline model

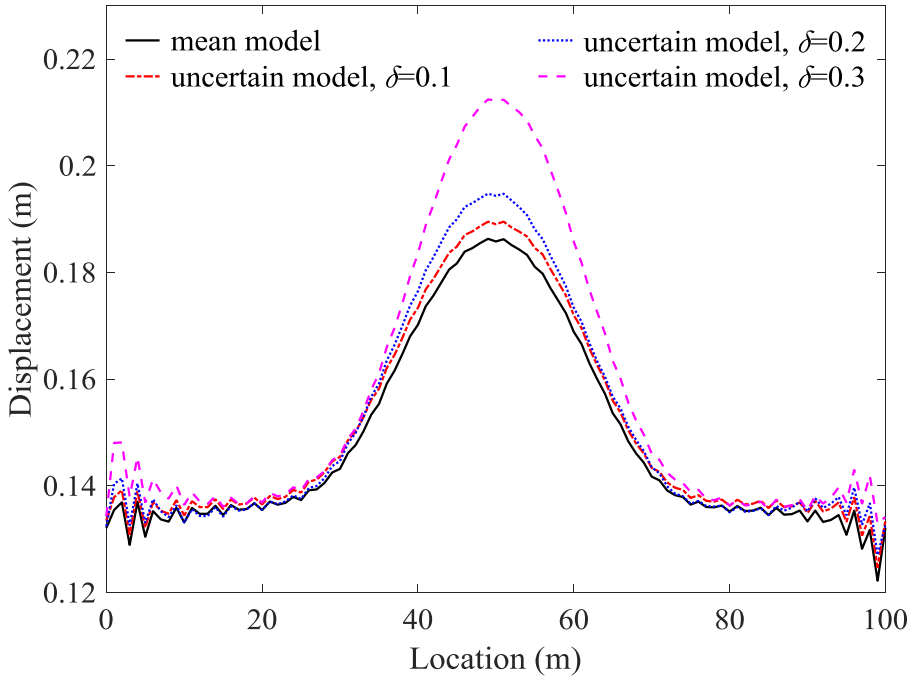

(a) Permanent contact model

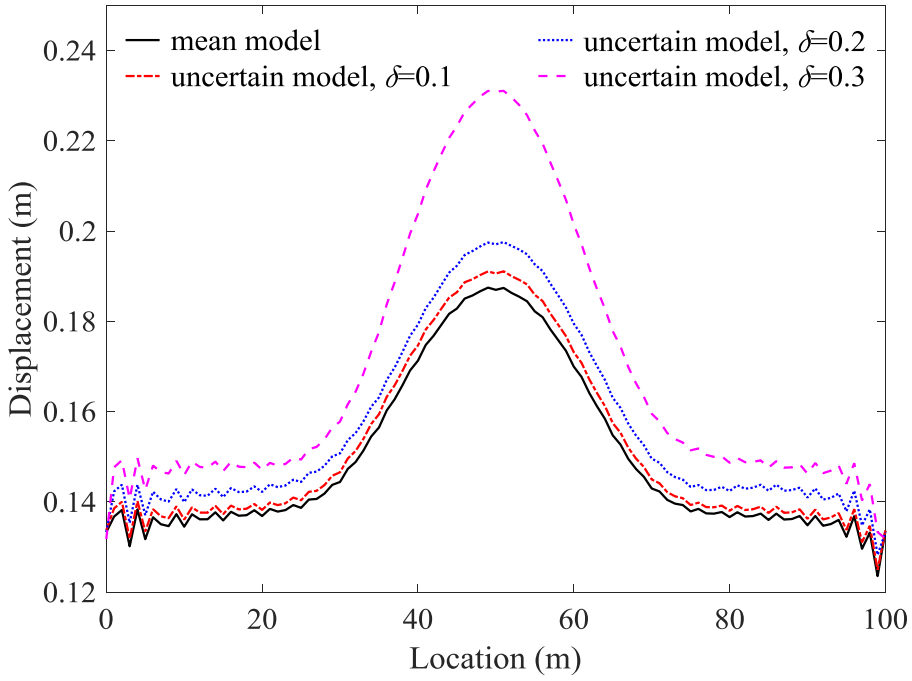

(b) Unilateral contact model

Fig. 12 Mean values of the maximum responses of the pipeline

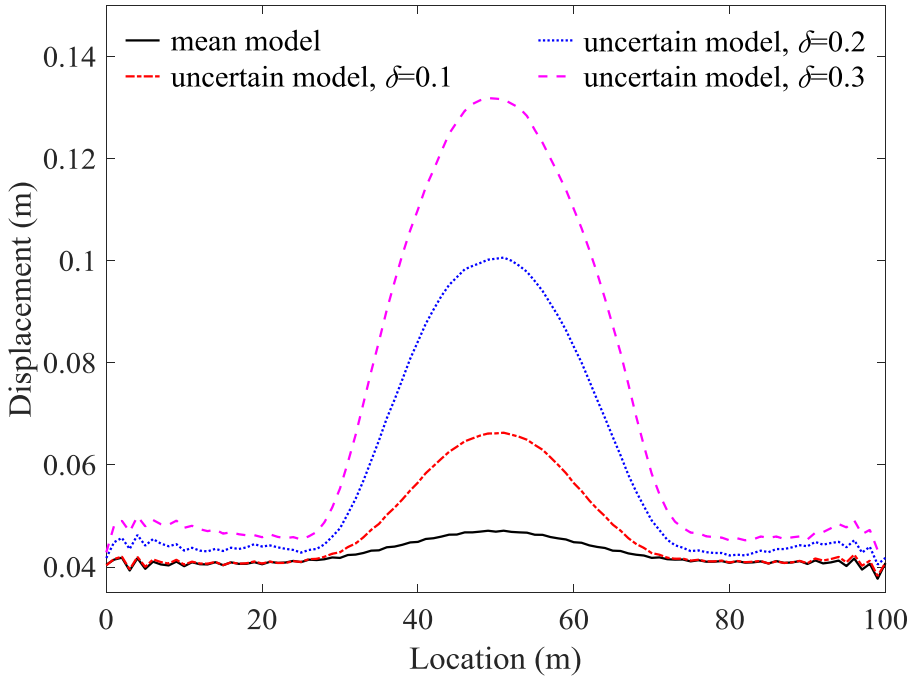

(a) Permanent contact model

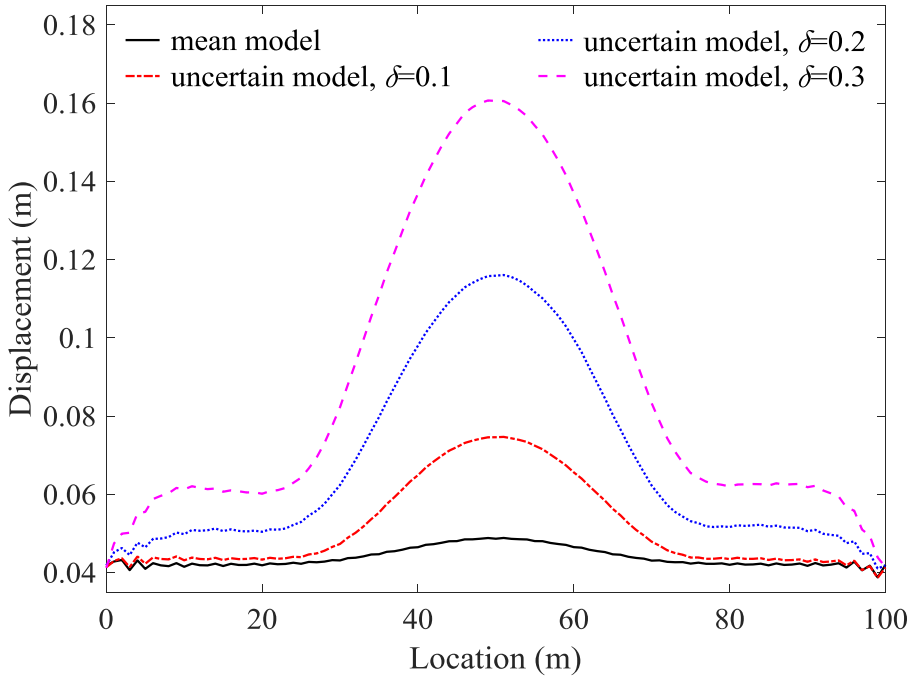

(b) Unilateral contact model

Fig. 13 Standard deviations of the maximum responses of the pipeline

pipeline are assumed to be rigid and hence their motions are equal to the ground motions, which are independent of the uncertainties of the pipeline. Secondly, the permanent contact model has a larger system stiffness than the unilateral contact model due to the total constraint of the seabed. Hence, in the permanent contact model, motions of the pipeline near the end supports are to a great extent controlled by the motions of the end supports. But in the unilateral contact model, the effect of end supports is much smaller.

5 Conclusions

This paper presents a computational model for the random vibration analysis of a subsea pipeline subjected to an earthquake. The randomness of the earthquake and modelling uncertainties of the pipeline are included in this computational model. Meanwhile, the spatial variation of the ground motions and the unilateral contact relationship between the pipeline and seabed are considered. Based on the present computational model, propagations of the randomness and modelling uncertainties are investigated through three representative cases. Results indicate that both the randomness of the earthquake and modelling uncertainties of the pipeline have significant influences on the random responses of the pipeline, and hence they should be considered in any earthquake analysis of the pipeline. Furthermore, comparative studies are performed between the permanent and unilateral contact models and remarkable differences are observed in their random responses. For the permanent contact model, random responses

601 of the pipeline exhibit a consistent statistical characteristic with the randomness and
602 modelling uncertainties, whereas for the unilateral contact model random responses are
603 more dispersed. These differences demonstrate the necessity of consideration of the
604 unilateral contact effect in the random earthquake analysis of subsea pipelines, especially
605 for those unburied or not anchored in deep sea regions.
606

607 # Acknowledgments

608 This authors wish to acknowledge the financial support from the National Basic
609 Research Program of China (2014CB046803), the National Science Foundation of China
610 (11672060), and the Cardiff University Advanced Chinese Engineering Centre.
611

612 # References

613 [1] Ghanem RG, Spanos PD. Stochastic Finite Element: A Spectral Approach. Springer-
614 Verlag; 1991.
615 [2] Schuëller GI, Pradlwarter HJ. Uncertain linear systems in dynamics: Retrospective
616 and recent developments by stochastic approaches. Eng Struct 2009; 31(11): 2507-
617 2517.
618 [3] Stefanou G. The stochastic finite element method: past, present and future. Comput
619 Methods Appl Mech Eng 2009; 198(9-12): 1031-1051.
620 [4] Singh BN, Lal A, Kumar R. Nonlinear bending response of laminated composite

plates on nonlinear elastic foundation with uncertain system properties. Eng Struct 2008; 30(4): 1101-1112.

[5] Fabro AT, Ferguson NS, Jain T, Halkyard R, Mace BR. Wave propagation in one-dimensional waveguides with slowly varying random spatially correlated variability. J Sound Vib 2015; 343(4): 20-48.

[6] Soize C. A nonparametric model of random uncertainties for reduced matrix models in structural dynamics. Probabilist Eng Mech 2000; 15(3): 277-294.

[7] Soize C. Random matrix theory and non-parametric model of random uncertainties in vibration analysis. J Sound Vib 2003; 263(4): 893-916.

[8] Chebli H, Soize C. Experimental validation of a nonparametric probabilistic model of nonhomogeneous uncertainties for dynamical systems. J Acoust Soc Am 2004; 115(2): 697-705.

[9] Duchereau J, Soize C. Transient dynamics in structures with non-homogeneous uncertainties induced by complex joints. Mech Syst Signal Process 2006; 20(4): 854-867.

[10] Adhikari S, Pastur L, Lytova A, Du Bois J. Eigenvalue density of linear stochastic dynamical systems: A random matrix approach. J Sound Vib 2012; 331(5): 1042-1058.

[11] Capiez-Lernout E, Soize C, Mignolet MP. Post-buckling nonlinear static and dynamical analyses of uncertain cylindrical shells and experimental validation.

641 Comput Methods Appl Mech Eng 2014; 271: 210-230.
642 [12] Capiez-Lernout E, Pellissetti M, Pradlwarter H, Schuëller GI, Soize C. Data and
643 model uncertainties in complex aerospace engineering systems. J Sound Vib 2006;
644 295(3-5): 923-938.
645 [13] Pellissetti M, Capiez-Lernout E, Pradlwarter H, Soize C, Schuëller GI. Reliability
646 analysis of a satellite structure with a parametric and a non-parametric probabilistic
647 model. Comput Methods Appl Mech Eng 2008; 198(2): 344-357.
648 [14] Gan C, Wang Y, Yang S, Cao Y. Nonparametric modeling and vibration analysis of
649 uncertain Jeffcott rotor with disc offset. Int J Mech Sci 2014; 78: 126-134.
650 [15] Ritto TG, Soize C, Sampaio R. Non-linear dynamics of a drill-string with uncertain
651 model of the bit–rock interaction. Int J Nonlin Mech 2009; 44(8): 865-876.
652 [16] Newland DE. An Introduction to Random Vibrations, Spectral and Wavelet Analysis.
653 Longman; 2012.
654 [17] Bi K, Hao H. Modelling and simulation of spatially varying earthquake ground
655 motions at sites with varying conditions. Probabilist Eng Mech 2012; 29: 92-104.
656 [18] Zhang YH, Li QS, Lin JH, Williams FW. Random vibration analysis of long-span
657 structures subjected to spatially varying ground motions. Soil Dyn Earthq Eng 2009;
658 29(4): 620-629.
659 [19] Tian L, Gai X, Qu B, Li H, Zhang P. Influence of spatial variation of ground motions
660 on dynamic responses of supporting towers of overhead electricity transmission

661 systems: An experimental study. Eng Struct 2016; 128: 67-81.
662 [20] Bilici Y, Bayraktar A, Soyluk K, Haciefendioğlu K, Ateş Ş, Adanur S. Stochastic
663 dynamic response of dam-reservoir-foundation systems to spatially varying
664 earthquake ground motions. Soil Dyn Earthq Eng 2009; 29(3): 444-458.
665 [21] Soliman HO, Datta TK. Response of overground pipelines to random ground motion.
666 Eng Struct 1996; 18(7): 537-545.
667 [22] Xu T, Lauridsen B, Bai Y. Wave-induced fatigue of multi-span pipelines. Mar Struct
668 1999; 12(2): 83-106.
669 [23] Sollund HA, Vedeld K, Fyrileiv O. Modal response of short pipeline spans on partial
670 elastic foundations. Ocean Eng 2015; 105: 217-230.
671 [24] Zeinoddini M, Parke GAR, Sadrossadat SM. Free-spanning submarine pipeline
672 response to severe ground excitations: water-pipeline interactions. J Pipeline Syst
673 Eng Prac 2012; 3(4): 135-149.
674 [25] Vedeld K, Sollund H, Hellesland J. Free vibrations of free spanning offshore
675 pipelines. Eng Struct, 2013; 56: 68-82.
676 [26] Païdoussis MP, Li GX. Pipes conveying fluid: a model dynamical problem. J Fluid
677 Struct 1993; 7(2): 137-204.
678 [27] Morison JR, Johnson JW, Schaaf SA. The force exerted by surface waves on piles. J
679 Petrol Technol 1950; 2(5): 149-154.
680 [28] Zhai H, Wu Z, Liu Y, Yue Z. Dynamic response of pipeline conveying fluid to random

681 excitation. Nucl Eng Des 2011; 241(8): 2744-2749.
682 [29] Mignolet MP, Soize C. Stochastic reduced order models for uncertain geometrically
683 nonlinear dynamical systems. Comput Methods Appl Mech Eng 2008; 197(45-48):
684 3951-3963.
685 [30] Shinozuka M. Monte Carlo solution of structural dynamics. Comput Struct 1972;
686 2(5-6): 855-874.
687 [31] Li Y, Zhang Y, Kennedy D. Reliability analysis of subsea pipelines under spatially
688 varying ground motions by using subset simulation. Reliab Eng Syst Saf 2018; 172:
689 74-83.
690 [32] Det Norsk Veritas. Submarine Pipeline Systems, DNV-OS-F101, 2007.
691 [33] Clough RW, Penzien J. Dynamics of Structures. McGraw-Hill; 1993.
692 [34] Dumanogluid AA, Soyluk K. A stochastic analysis of long span structures subjected
693 to spatially varying ground motions including the site-response effect. Eng Struct
694 2003; 25(10): 1301-1310.
695 [35] Berg GV, Housner GW. Integrated velocity and displacement of strong earthquake
696 ground motion. B Seismol Soc Am 1961; 51(2): 175-189.
697 [36] Desceliers C, Soize C, Cambier S. Non-parametric-parametric model for random
698 uncertainties in non-linear structural dynamics: Application to earthquake
699 engineering. Earthq Eng Struct Dyn 2004; 33(3): 315-327.
700